AJBMS AFGHANISTAN Journal of Basic Medical Sciences
ISSN: 3005-6632

Afghanistan Journal of Basic Medical Sciences

2026 Jan; 3(1): 38-52.

ajbms.knu.edu.af

Unraveling the Molecular Mechanism of Curcumin Inhibition against White Spot Syndrome Virus VP26: An Integrated Computational Study

Ahmad Wali Ataye [1,2], Nasir Nazari [3,4], Mahdi Nowroozi [3,4], Ghulam Aishan Sabawoon[5], Nooh Amin [3,4], *Dawood Hossaini [4], Aziz-ur-Rahman Niazi [1,6]

1. *Department of Public Health, Faculty of Medicine, Afghan International Islamic University of Kabul, Afghanistan*
2. *Department of Microbiology, Faculty of Allied Science, Kabul University of Medical Science, Kabul, Afghanistan.*
3. *Medical Research and Technology Center, Khatam Al-Nabieen University, Kabul, Afghanistan*
4. *Department of Paraclinical Sciences and Laboratory Management, Faculty of Medical Laboratory Technology, Khatam Al-Nabieen University, Kabul, Afghanistan*
5. *Pharmacology department, Faculty of pharmacy, Shifa University, Kabul, Afghanistan*
6. *Department of Public Health and Infectious Diseases, Faculty of Medicine, Herat University, Herat, Afghanistan*

ARTICLE INFO

Type: Original Article

Received: 4 Dec, 2025

Accepted: 29 Dec, 2025

*Corresponding Author:
E-mails:
dawood.hossaini@knu.edu.af
Dawoodhossaini75@gmail.com

To cite this article:

Ataye AW, Nazari N, Nowroozi M, Sabawoon GA, Amin N, Hossaini D, Niazi AR. Unraveling the molecular mechanism of curcumin inhibition against white spot syndrome virus VP26: an integrated computational study. Afghanistan Journal of Basic Medical Sciences. 2026 Jan;3(1):38–52.

DOI:
https://doi.org/10.62134/khatamuni.143

ABSTRACT

Background: The White Spot Syndrome Virus (WSSV) poses a significant threat to global shrimp aquaculture, necessitating the development of effective antiviral agents. Among the structural proteins of WSSV, VP26 plays a critical role in viral assembly and host-cell interactions, making it a promising target for therapeutic intervention. Curcumin, a bioactive compound derived from Curcuma longa, exhibits broad-spectrum antiviral potential, but its molecular mechanism of inhibition against WSSV remains unclear.

Methods: An integrated computational approach combining molecular docking and molecular dynamics (MD) simulations was employed to elucidate the inhibitory interactions between curcumin and VP26.

Results: Docking results revealed a favorable binding affinity of –6.53 kcal/mol, indicating a spontaneous and stable interaction predominantly stabilized by van der Waals forces and hydrogen bonding, particularly involving Arg136. Subsequent 100 ns MD simulations demonstrated that the VP26-curcumin complex maintained high structural stability, with consistent hydrogen bonding, short interatomic distances, and minimal deviation in the radius of gyration. Residue-specific flexibility analysis indicated localized increases in dynamics near the binding site, suggesting subtle conformational adaptation upon ligand binding. The MM/PBSA binding free energy (-93.46 kJ/mol) confirmed strong and stable complex formation.

Conclusion: Collectively, these findings provide atomistic insights into the binding mechanism of curcumin with VP26, supporting its potential as a natural antiviral inhibitor against WSSV and offering a foundation for the rational design of novel antiviral agents in aquaculture.

Keywords: White Spot Syndrome Virus, Curcumin, Molecular Docking, Molecular Dynamics Simulations

Introduction

The White Spot Syndrome Virus (WSSV) is a highly virulent pathogen and the etiological agent of White Spot Disease, a condition responsible for devastating economic losses in global shrimp aquaculture (1, 2). As a member of the Nimaviridae family, WSSV possesses one of the largest known viral genomes, a circular double-stranded DNA exceeding 300 kilobases that encodes for approximately 180 proteins (3-5). Among these, the structural proteins VP19, VP24, VP26, and VP28 are critically involved in viral assembly and host-cell interactions, making them promising targets for antiviral strategies (6).

The search for effective therapeutics has increasingly turned towards natural products, which are a rich source of bioactive compounds with diverse pharmacological properties (7, 8). Curcumin, the primary curcuminoid derived from the rhizome of Curcuma longa L. (turmeric), is a prime example. This poly phenolic compound has garnered significant attention for its broad-spectrum biological activities, including potent anti-oxidant, anti-inflammatory, and anti-cancer effects (9, 10). Notably, its antiviral potential has been demonstrated against a range of viruses, suggesting a mechanism that may involve the disruption of viral entry or replication (11-13). Despite this promise, the precise molecular interactions between curcumin and specific viral targets remain largely unexplored. Experimental elucidation of these interactions can be resource intensive, highlighting the value of robust computational methods as a preliminary investigative tool (14). Integrated computational approaches, particularly molecular docking paired with molecular dynamics (MD) simulations, offer a powerful strategy to predict ligand-binding modes, characterize binding affinities, and evaluate the stability of resulting complexes under physiological conditions (15, 16). Molecular docking provides a static snapshot of potential binding poses, while MD simulations extend this insight by modeling the dynamic behavior and conformational stability of the protein-ligand complex over time. Given the critical role of the VP26 protein in WSSV pathogens and the documented antiviral properties of curcumin, we hypothesize that curcumin may act as a potent inhibitor of VP26.

To test this hypothesis, we employed an integrated in silico approach combining molecular docking and extensive MD simulations. Our objectives were to: 1) predict the binding affinity and precise binding pose of curcumin within the VP26 structure, 2) identify the key amino acid residues mediating this interaction, and 3) assess the stability and dynamic behavior of the curcumin-VP26 complex. The findings from this study provide crucial atomistic insights into the inhibitory mechanism of curcumin against WSSV, establishing a foundational framework for the future development of targeted antiviral agents in aquaculture.

Methods

Protein Preparation

The three-dimensional structure of the (WSSV) VP26 protein was retrieved from the Protein Data Bank (PDB ID: 2EDM). Protein preparation was conducted using AutoDockTools 1.5.6 program (9). The preparation process involved removing all hetero atoms and crystallographic water molecules, adding hydrogen atoms, and assigning Gasteiger partial charges. The resulting structure was subsequently saved in the PDBQT format for docking analysis.

Ligand Preparation and Binding Site Prediction

The three-dimensional structure of curcumin (PubChem CID: 969516) was obtained from the

PubChem database (17). The ligand geometry was optimized using the Gaussian software package (18) with the B3LYP/6-31G basis set to achieve a stable conformation.

Molecular Docking

Molecular docking studies were carried out to explore the binding affinity and interaction pattern between curcumin and the VP26 protein using AutoDock 4.2 (8). A grid box with dimensions of 60 × 60 × 80 and a grid spacing of 0.375 Å was defined to encompass the predicted binding pocket. The docking procedure was performed with 200 independent runs using the Lamarckian Genetic Algorithm (LGA). During docking, the protein was kept rigid, while all rotatable bonds in the ligand were allowed to move freely. The most favorable docking conformation, defined as the structure with the lowest binding energy in the most populated cluster, was selected for further analysis. Intermolecular interactions, including hydrogen bonds and van der Waals contacts, were visualized and analyzed using Ligplot+ program (19).

Molecular Dynamics (MD) Simulation

To evaluate the stability and dynamic behavior of the VP26-curcumin complex, MD simulations were performed using GROMACS 2022.6 (20) with the AMBER99SB force field. Topology parameters for curcumin were generated using the ACPYPE Python interface (21). Two systems were simulated: the VP26–curcumin complex and the free VP26 protein. Systems were solvated in a cubic periodic box filled with TIP3P water molecules, maintaining a minimum distance of 1.0 nm between the solute and the box boundaries. System neutrality was achieved by adding appropriate numbers of Na^+ and Cl^- counterions, followed by adjustment to a physiological salt concentration of 0.15 M. Energy minimization was performed using the steepest descent algorithm until the maximum force was reduced below 100 kJ/mol/nm. The minimized system was equilibrated in two stages. NVT equilibration (canonical ensemble) for 1 ns at 310 K using the Nose–Hoover thermostat. NPT equilibration (isothermal–isobaric ensemble) for 1 ns at 1 bar using the Parrinello–Rahman barostat. A production MD run was then performed for 100 ns with a 2-fs time step.

Results and Discussion

Docking Analysis of the Curcumin-VP26 Complex

Molecular docking analysis using AutoDock predicted a stable binding mode for curcumin within a defined pocket of the VP26 protein. The calculated binding affinity for the most favorable pose was -6.53 kcal/mol, corresponding to a predicted inhibition constant (Ki) of 16.34 µM (Table 1). This energetically favorable score suggests a spontaneous and stable binding interaction under physiological conditions.

Table 1: Energetic components of the curcumin-VP26 interactions obtained from molecular docking

Lowest binding energy (kcal/mol)	*Inhibition constant (Micro Molar)*	*vdW + H- bond + dissolved energy (kcal/mol)*	*electrostatic energy (kcal/mol)*	*Torsional Free Energy (kcal/mol)*
- 6.53	16.34	- 9.16	- 0.36	2.98

A detailed decomposition of the binding energy revealed that the interaction was primarily stabilized by van der Waals forces, hydrogen bonding, and desolvation effects, which collectively contributed -9.16 kcal/mol. In contrast, the electrostatic contribution was relatively minor at -0.36 kcal/mol. The torsional free energy penalty, associated with the loss of conformational freedom upon binding, was +2.98 kcal/mol.

The binding orientation of curcumin, illustrated in Fig. 1, shows the ligand nestled within a hydrophobic cleft of the VP26 protein. Analysis of the specific molecular interactions identified several key amino acid residues forming van der Waals contacts with curcumin, including Tyr46, Asp47, Gln48, Met49, Pro72, Asp132, Thr134, Arg136, Asn186, and Gly188. A critical stabilizing feature of the complex is a conventional hydrogen bond formed between the guanidino group of Arg136 and the carbonyl oxygen atom of curcumin. This specific interaction, combined with the extensive network of non-bonded contacts, underscores the binding of curcumin to the VP26 binding site and provides a structural rationale for its potential inhibitory activity.

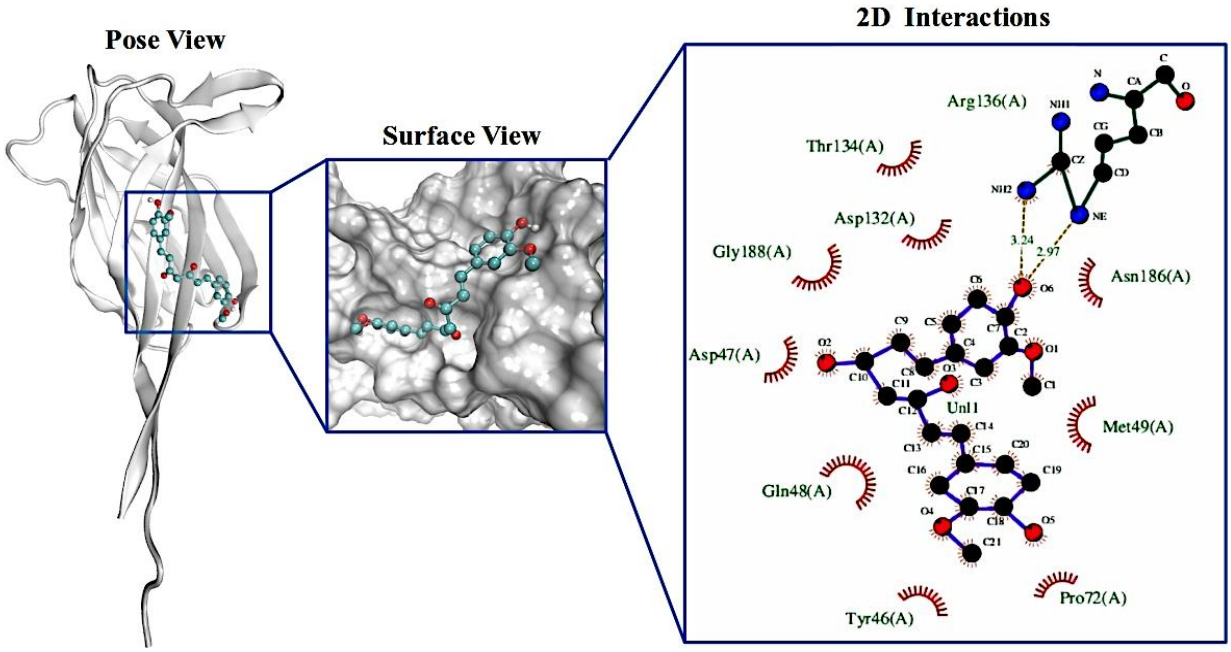

Fig. 1: Predicted binding pose of curcumin in the binding site of VP26 protein. The three-dimensional binding pose of curcumin within the surface representation of the VP26 binding pocket and two-dimensional ligand-protein interaction diagram generated by Ligplot^{+}, detailing the key intermolecular contacts

The binding affinity observed for curcumin against VP26 is comparable to other reports of curcumin's interactions with viral and protein targets. For example, in silico studies targeting viral proteases and coat proteins of plant viruses reported curcumin docking energies in the range of −6.3 to −7.2 kcal/mol, indicating similar moderate binding strengths to viral structural proteins in silico (−7.2 kcal/mol for PVY coat protein) (22). Similar docking studies against human disease-related proteins also report curcumin binding energies in a range that supports its potential as a modest affinity inhibitor (e.g., docking to SARS-CoV-2 proteins and CDK2 in cancer studies) (23). These comparative studies suggest that curcumin tends to show consistent moderate binding affinities across diverse protein targets, reinforcing the hypothesis that curcumin can interact reliably with protein pockets through hydrophobic and hydrogen-bonding interactions. The dominant contribution of van

der Waals and hydrogen bonding observed in our analysis is in agreement with these previous reports where hydrophobic contacts play central roles in stabilizing complexes of curcumin with viral domains and enzymes (24).

Molecular Dynamics Simulation Analysis

To validate the stability of the docked curcumin-VP26 complex and gain deeper insights into the molecular dynamics and structural consequences of binding, we performed 100 ns MD simulations for both the ligand-bound (VP26-Curcumin) and unbound (Free VP26) states.

Structural and Dynamical Analysis

The structural integrity and global dynamics of VP26 in its free and curcumin-bound states were rigorously assessed by calculating the Root Mean Square Deviation (RMSD), Root Mean Square Fluctuation (RMSF), Radius of gyration (Rg), secondary structure composition, and through Principal Component Analysis (PCA). These metrics collectively provide a comprehensive view of the protein's stability, flexibility, and conformational landscape. The backbone RMSD analysis, depicted in Fig. 2, revealed the dynamic stability of both systems throughout the simulation. After an initial equilibration period, the Free VP26 structure stabilized, maintaining an average RMSD of 0.446 ± 0.039 nm.

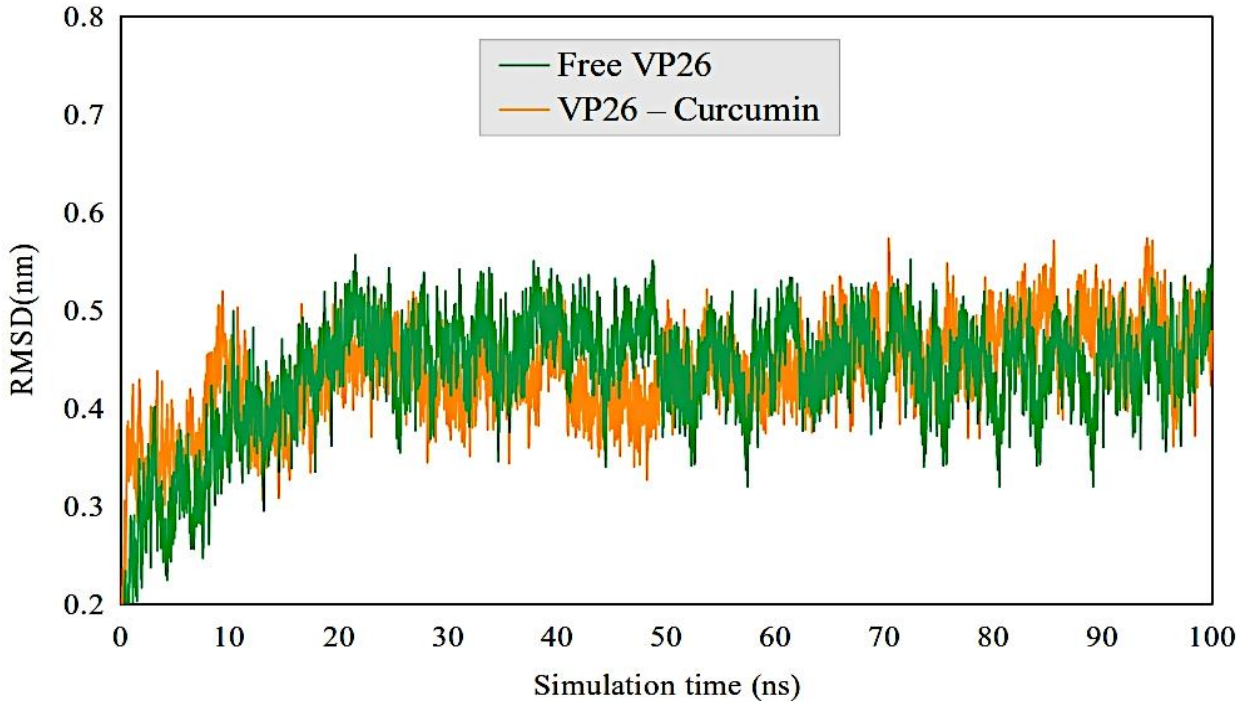

Fig. 2: Backbone RMSD of trajectories of Free VP26 and the VP26-Curcumin complex over the 100 ns MD simulation

The preservation of global compactness, as evidenced by nearly unchanged radius of gyration (Rg) values between Free VP26 and the VP26-Curcumin complex, further supports that curcumin binding does not disrupt the native fold of VP26. Similar result has been reported in MD studies of curcumin-related ligand complexes, where stable Rg profiles

were observed for both unbound and ligand-bound forms throughout 100 ns trajectories, indicating that ligand engagement does not lead to major conformational expansion or unfolding but rather maintains overall structural integrity (25).

A key observation emerges from the VP26-Curcumin complex, which settled into a distinct, stable state with a consistently higher average RMSD of 0.479 ± 0.033 nm (Table 2). This elevation in RMSD does not signify instability or unfolding, but rather indicates a subtle ligand-induced structural perturbation. Curcumin binding has shifted the protein's energy landscape, stabilizing a new conformational state that is slightly different from its native, unbound form. The well-defined plateau and low standard deviation in the complex's trajectory are critical, as they confirm that this altered conformation is itself stable and persistent. This represents the formation of a specific and well-defined ligand-protein complex, where VP26 has undergone a minor but stable structural adaptation to accommodate curcumin. This behavior is consistent with previous MD analyses demonstrating that ligand engagement can shift a protein's energy landscape into a new conformational basin without compromising overall stability, leading to an alternative but stable structural sub-state sampled during the trajectory (25).

Table 2: Comparative summary of MD simulation parameters for the Free VP26 and VP26-Curcumin complex. Values represent the mean ± standard deviation calculated over the stable trajectory (last 20 ns)

System	*Mean RMSD (nm)*	*Mean RMSF (nm)*	*Mean Rg (nm)*
Free Vp26	0.446±0.039	0.139±0.088	1.697±0.016
Vp26 – Curcumin	0.479±0.033	0.143±0.089	1.671±0.016

To dissect the local flexibility changes upon binding, we analyzed the per-residue RMSF (Fig. 3). While the overall mean RMSF values were similar (0.139 ± 0.088 nm for Free VP26 vs. 0.143 ± 0.089 nm for the complex), a residue-specific analysis reveals critical, localized effects that provide deep insight into the binding mechanism.

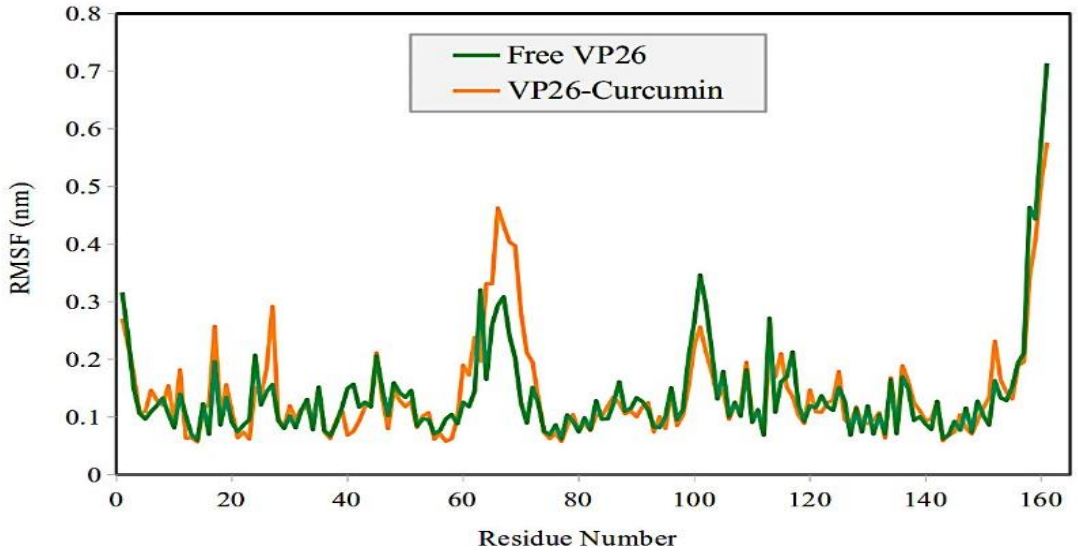

Fig. 3: Per-residue RMSF of Free VP26 and the VP26-Curcumin complex

Contrary to the typical expectation of rigidification at a binding site, we observed a significant increase in flexibility for several key residues directly involved in the interaction with curcumin. Most notably, Arg136, which forms a critical hydrogen bond with the ligand, shows a marked increase in fluctuation (0.170 nm in Free VP26 vs. 0.189 nm in the complex). The hydrogen bond with Arg136, while stable, appears to be dynamic in nature, pulling the residue into a new conformational sub-state that exhibits greater mobility than in the unbound protein.

This localized increase in flexibility was not isolated. A pronounced enhancement in dynamics was also observed in the adjacent loop region spanning residues 60-75**,** which contained the binding site residue Pro72. Furthermore, the N-terminal region (residues 25-30) also becomes more flexible. These data paint a picture of a binding event that induces strain or dynamic allostery in its immediate vicinity.

The potential impact of this binding induced dynamic adaptation on the global compactness of VP26 was assessed by monitoring the Rg, as shown in Fig. 4.

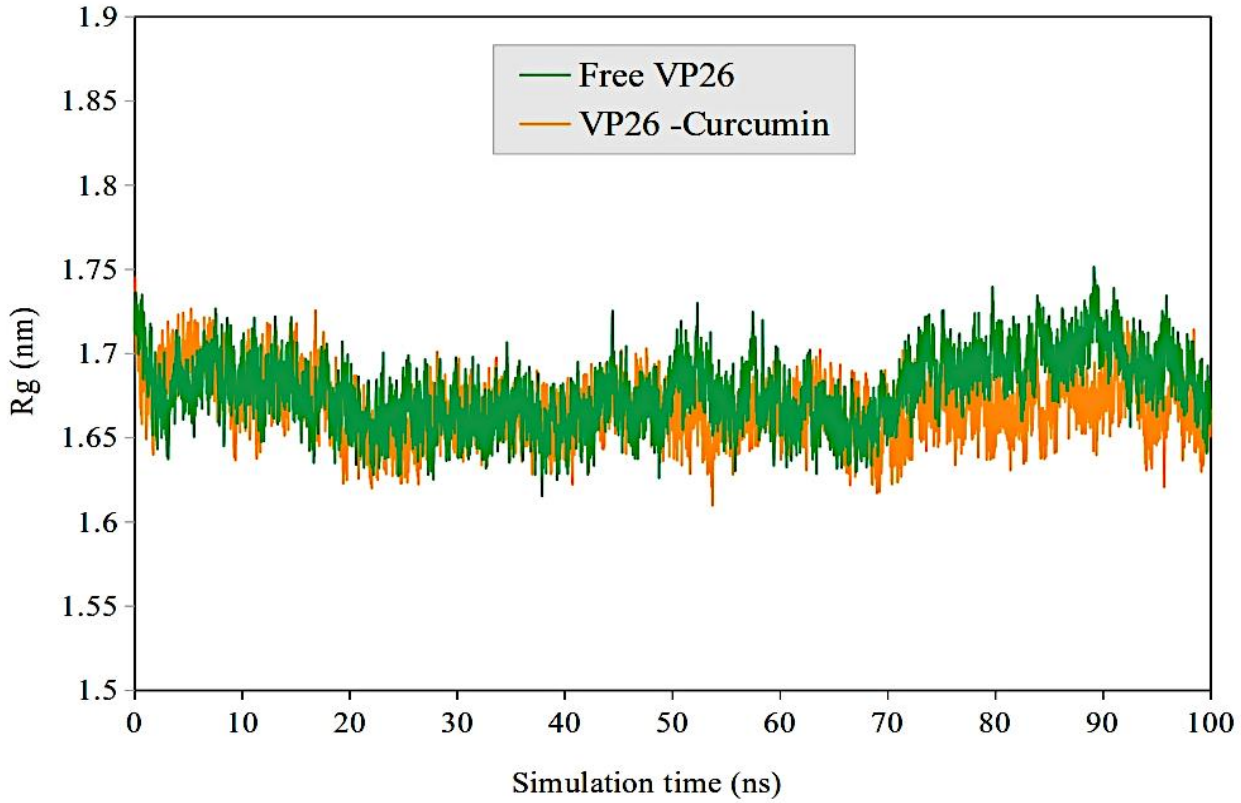

Fig. 4: Rg plots for Free VP26 and the VP26-Curcumin complex

Such localized increases in fluctuation at or near ligand interaction sites are consistent with previous reports showing that ligand binding does not universally rigidify a protein but can instead induce region-specific changes in flexibility. For example, MD studies comparing ligand-bound and unbound protein structures have demonstrated that binding can increase mobility in certain loops or side chains adjacent to the binding site, reflecting a dynamic adaptation of the protein to accommodate the ligand rather than a simple rigidification of the

binding interface (26). Furthermore, models of ligand-protein dynamics have shown that ligand engagement often leads to compensatory flexibility changes whereby regions directly interacting with the ligand become more dynamic while other regions may become less so, illustrating the complex and sometimes counterintuitive nature of protein flexibility upon binding (27). These observations support our interpretation that curcumin binding induces localized dynamic adaptation in VP26, particularly in loop regions and binding site residues, which may be part of the mechanism by which the protein accommodates ligand binding without global destabilization.

The average Rg for the Free VP26 system was calculated to be 1.697 ± 0.016 nm, while the VP26-Curcumin complex exhibited a very similar average Rg of 1.671 ± 0.016 nm. This minor difference suggests that the structural perturbation and localized flexibility changes do not translate into a major conformational expansion or compaction of the overall protein fold. The stability of the complex is further underscored by the identical and minimal standard deviation of the Rg, indicating a consistent and well-packed global structure throughout the simulation, despite the increased fluctuations at specific sites. The nearly identical Rg values observed for the Free VP26 and VP26–Curcumin systems indicate that ligand binding does not induce significant global expansion or compaction of the protein. In molecular dynamics simulations, Rg is a direct measure of protein compactness, and stable Rg values over time are interpreted as preservation of the overall tertiary structure despite local conformational fluctuations (28).

To assess whether curcumin binding induced significant alterations in the protein's secondary structure, we analyzed the average percentage of each secondary structure element throughout the simulation (Fig. 5).

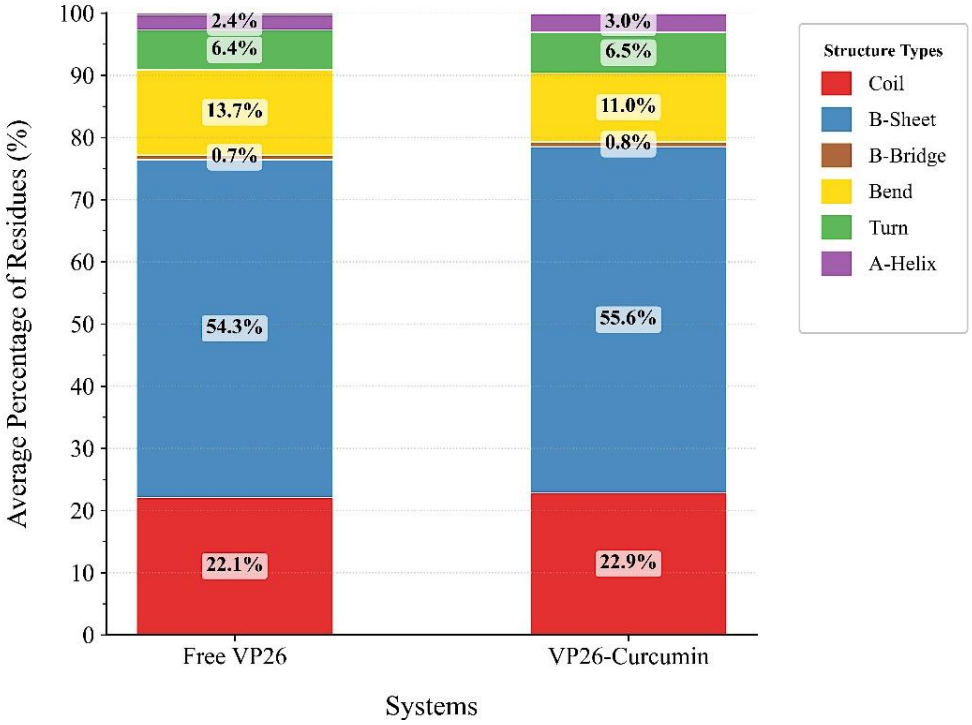

Fig. 5: Average percentage of the secondary structure composition of Free VP26 and the VP26-Curcumin complex throughout the last 20 ns MD simulation

The overall composition was highly conserved between the Free VP26 and the VP26-Curcumin complex. B-Sheet (54.3% vs. 55.6%) and Coil (22.1% vs. 22.9%) remained the dominant structural elements in the free and bound states, respectively, indicating that no large-scale unfolding or refolding occurred. Minor fluctuations were observed in other elements: A-Helix content increased from 2.4% to 3.0%, B-Bridge from 0.7% to 0.8%, and turn from 6.4% to 6.5%. Conversely, a decrease was noted in Bend content, from 13.7% to 11.0%. Given the subtle nature of these changes, they do not point to a drastic structural reorganization. Instead, they likely reflect localized adjustments and a slight stabilization of certain elements, particularly B-sheets, upon ligand binding, which may contribute to the overall stability of the complex without fundamentally altering the protein's core architecture.

To understand the effect of curcumin binding on the large-scale motions of the VP26, we performed Principal Component Analysis. The analysis of the eigenvalues showed that the first two principal eigenvectors (PC1 and PC2) represent the most dominant collective motions in both systems (Figure 6a). The projection of the simulation trajectories onto these two eigenvectors revealed the conformational space sampled by the protein (Fig. 6b and c).

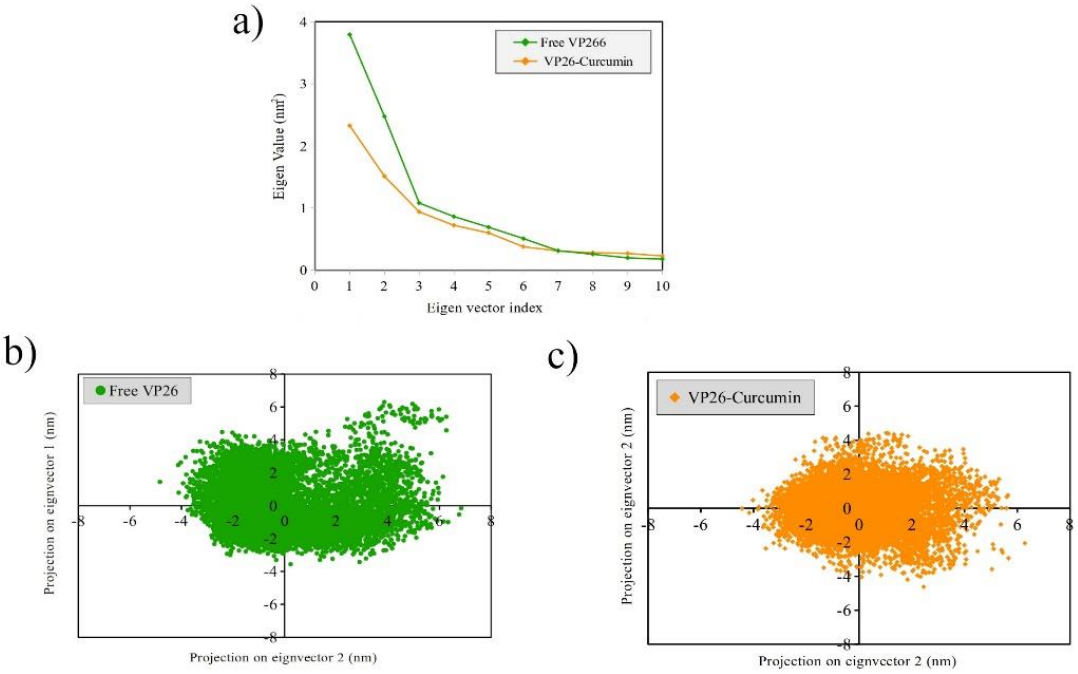

Fig. 6: Principal Component Analysis (PCA) of the MD trajectories. (a) Eigenvalue of the first 10 eigenvectors. Projection of the trajectory frames onto the phase space defined by the first two principal eigenvectors for (b) Free VP26 and (c) VP26-Curcumin complex

The Free VP26 system was characterized by a relatively broad distribution, indicating its inherent flexibility. The conformational ensemble of the VP26-Curcumin complex also samples a broad area, but with a subtle yet consistent shift and a slight narrowing of its density core compared to the free protein. This minor change in the conformational sampling suggests that the binding of curcumin induces a modest redistribution of the protein's essential

motions, stabilizing a specific conformational sub-ensemble. While the effect is not dramatic, this subtle modulation of global dynamics, when combined with the local changes observed in RMSF, may contribute to the mechanism of curcumin's interaction with VP26. Similar PCA-based MD analyses in the literature have been used to differentiate functional states of proteins, identify metastable substates, and compare conformational ensembles between unbound and ligand-bound forms, highlighting how ligand binding can alter the accessible conformational landscape while preserving overall structural integrity (29). These observations support our interpretation that curcumin binding subtly modulates collective motions of VP26, redistributing the conformational sampling without introducing large-scale destabilization.

Binding Stability and Interaction Analysis

To gain deeper insights into the stability of the curcumin-VP26 complex and the specific molecular interactions that govern binding, we analyzed the contact frequency, minimum distance, hydrogen bonding, and binding free energy throughout the MD simulation trajectory.

The stability of the curcumin-VP26 complex, initially predicted by molecular docking, was rigorously assessed during the 100 ns MD simulation. The number of atomic contacts between curcumin and VP26 residues provides a measure of the extent of the interaction interface. As shown in Fig. 7a, the complex maintained a high and stable number of contacts throughout the simulation.

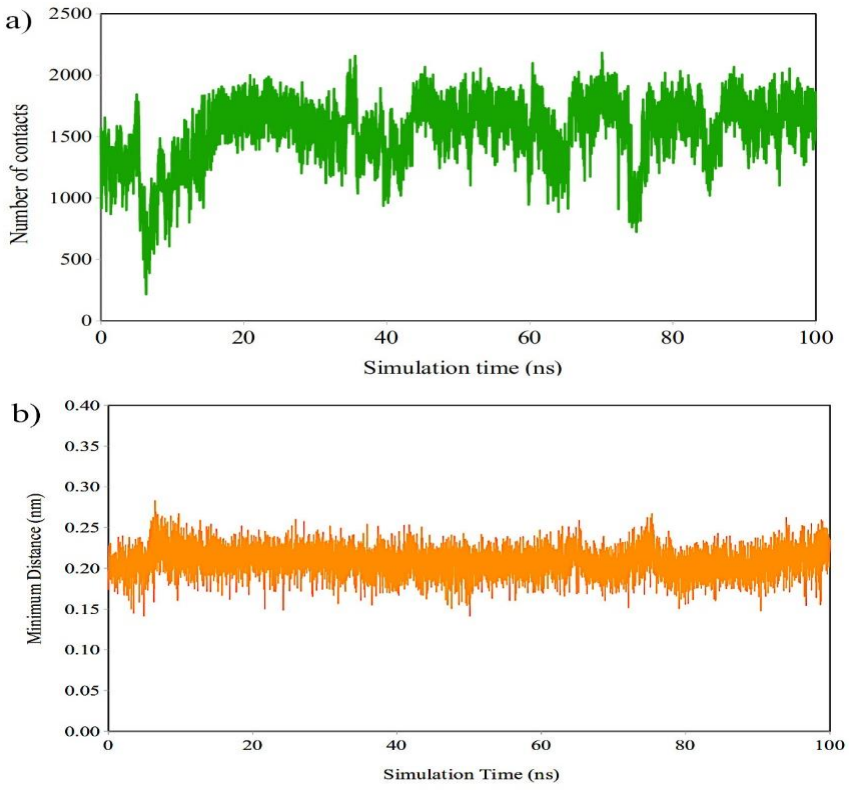

Fig. 7: Analysis of the atomic interactions and proximity in the curcumin-VP26 complex. **(a)** The time-evolution of the number of atomic contacts (cutoff distance 0.6 nm) between curcumin and VP26 residues throughout the 100 ns molecular dynamics simulation **(b)** The minimum distance between the curcumin molecule and the VP26 binding site over the simulation time

Quantitatively, the system exhibited an average of 1548 contacts, with a maximum of 2183 and a minimum of 215. The consistently high average and maximum values indicate a robust and dense network of interactions, suggesting the ligand is extensively engaged with the binding site residues. While the transient dips to a minimum of 215 contacts reflect the dynamic nature of the binding interface, where side chains sample different conformations, the rapid recovery to a high number of contacts underscores the resilience and enduring nature of the association. Such analyses of contact persistence as a marker of binding stability are commonly used to validate docking poses in MD studies, where a stable interaction network correlates with maintained complex integrity over time (30).

Complementing this, the minimum distance between the ligand and the protein binding pocket was analyzed as a critical metric for binding stability. As shown in Fig. 7b, the minimum distance between curcumin and the VP26 binding site remained consistently low throughout the simulation. The average minimum distance was calculated to be 0.21 nm, fluctuating within a very narrow range between 0.14 nm (min) and 0.28 nm (max). This consistently short proximity, far below a typical van der Waals cutoff, indicates that curcumin remained intimately associated and firmly positioned within its binding pocket without any significant dissociation events. The convergence of a high number of atomic contacts with a short and stable minimum distance provides strong, mutually reinforcing evidence for a tight and stable binding mode.

Hydrogen bonding plays a pivotal role in conferring specificity and strength to protein-ligand interactions. The analysis of hydrogen bond formation (Fig. 8) throughout the simulation trajectory revealed that the curcumin-VP26 complex maintained persistent hydrogen bonding.

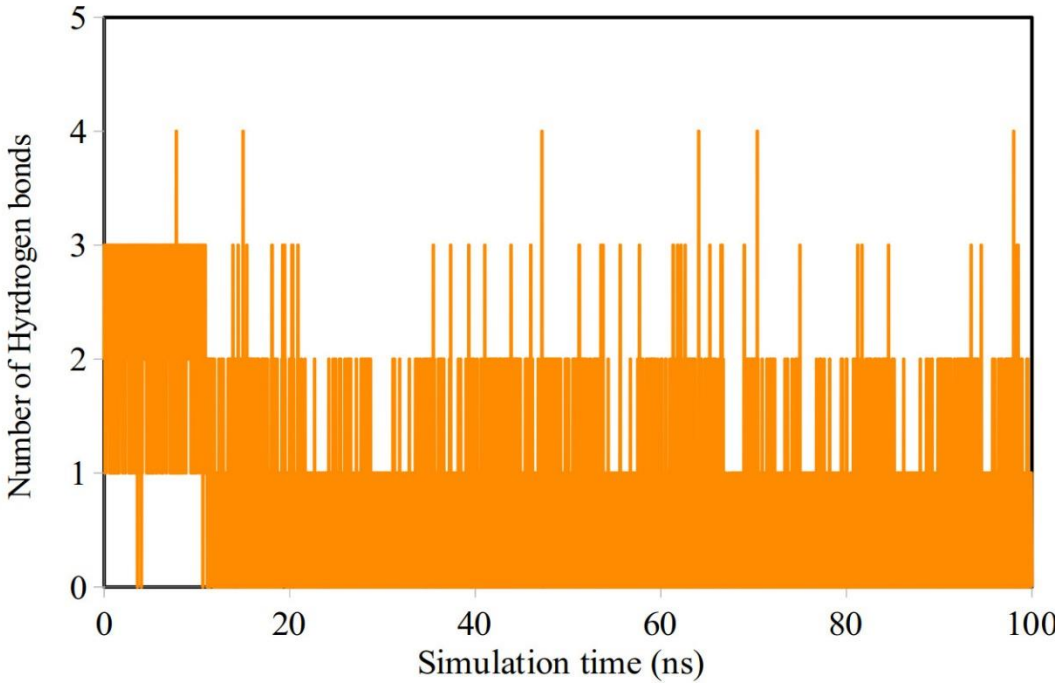

Fig. 8: Time-dependent evolution of the number of hydrogen bonds between curcumin and the VP26 protein during the 100 ns molecular dynamics simulation

The stability of the binding pose predicted by molecular docking was visually confirmed through a time evolution analysis of the simulation snapshots. As depicted in Fig. 9, representative structures extracted at 25 ns intervals (0, 25, 50, 75, and 100 ns) demonstrate that curcumin remains securely bound within the same hydrophobic pocket of VP26. The ligand's orientation and position are remarkably consistent from the initial frame to the final frame, with no significant translation or rotation observed. This visual evidence directly corroborates the quantitative data from the contact, and distance analyses, confirming that the initially docked pose is not an artifact but represents a genuine, stable binding mode.

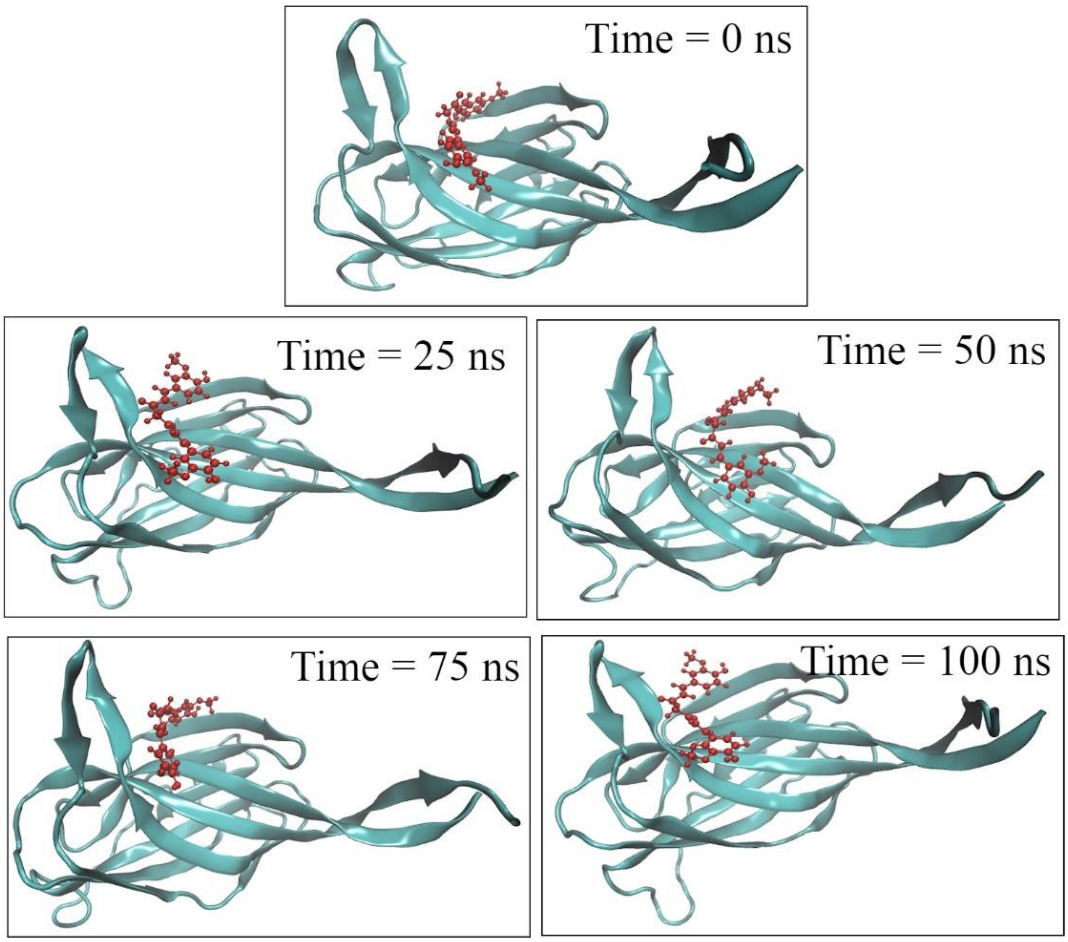

Fig. 9: Structural snapshots of the curcumin-VP26 complex at key time points (0, 25, 50, 75, and 100 ns) from the 100 ns molecular dynamics simulation. VP26 is shown in cartoon representation (cyan), curcumin is depicted as red ball and sticks

To quantitatively evaluate the binding affinity of curcumin for VP26, the Molecular Mechanics/Poisson-Boltzmann Surface Area (MM/PBSA) method was employed. The calculated binding free energies from the stable simulation trajectory are summarized in Table 3.

Table 3: MM/PBSA binding free energy components for the curcumin-VP26 complex (kJ/mol)

Energy Component	***Mean ± Standard Deviation***
van der Waals Energy	-128.253 ± 27.688
Electrostatic Energy	-7.684 ± 10.672
Polar Solvation Energy	57.371 ± 17.188
SASA Energy	-14.891 ± 2.503
Total Binding Energy	-93.457 ± 23.540

The MM/PBSA results reveal a strongly favorable binding free energy of -93.46 kJ/mol for the curcumin-VP26 complex. Decomposition of the total energy into its components shows that the binding is primarily driven by a large, favorable van der Waals contribution (-128.25 kJ/mol), supplemented by a favorable non-polar solvation energy (-14.89 kJ/mol). This indicates that hydrophobic interactions and the close shape complementarity between curcumin and the VP26 binding pocket are the dominant forces stabilizing the complex. While the electrostatic energy is favorable, its effect is largely counteracted by the unfavorable polar solvation penalty upon binding. This is a common phenomenon in biomolecular recognition, where the desolvation of charged/polar groups is energetically costly.

Conclusion

This study provides a molecular-level perspective on the potential interaction between curcumin and the VP26 protein of White Spot Syndrome Virus, highlighting curcumin's capacity to associate stably with a functionally relevant region of the protein. The integrated computational framework suggests that such binding may induce localized conformational and dynamic constraints that could plausibly influence VP26-mediated processes during viral infection. Importantly, these observations should be interpreted as mechanistic hypotheses rather than direct evidence of antiviral activity, as they are derived exclusively from in silico analyses. Nevertheless, the findings contribute to a conceptual understanding of how natural polyphenolic compounds might target structural viral proteins and offer a rational starting point for subsequent experimental validation, structure-based optimization, and biological assessment in the context of shrimp aquaculture disease management.

Acknowledgments

The authors extend their heartfelt appreciation to the Khatam Al-Nabieen University Medical Research and Technology Center for its supportive scientific environment, institutional backing, and access to essential research resources that made this narrative review possible.

Founding

None.

Conflict of interest

The authors declare that there is no conflict of interests.

Reference

1. Narasimman V, Ramachandran S. In silico analysis of low molecular weight sulfated chitosan from Sepia brevimana as potential inhibitors of white spot syndrome envelope proteins. Biomass Conversion and Biorefinery. 2024;14(16):18539-50.
2. Wu C, Yang F. Localization studies of two white spot syndrome virus structural proteins VP51 and VP76. Virol J. 2006;3(1):76.

3. Rozenberg A, Brand P, Rivera N, Leese F, Schubart CD. Characterization of fossilized relatives of the White Spot Syndrome Virus in genomes of decapod crustaceans. BMC Evolutionary Biol. 2015;15(1):142.
4. Cao X-T, Wu L-J, Xu F-L, Li X-C, Lan J-F. Pc Trim prevents early infection with white spot syndrome virus by inhibiting AP1-induced endocytosis. Cell Communication and Signaling. 2023;21(1):104.
5. Seok SH, Park JH, Cho SA, Baek MW, Lee HY, Kim DJ, et al. Cloning and sequencing of envelope proteins (VP19, VP28) and nucleocapsid proteins (VP15, VP35) of a white spot syndrome virus isolate from Korean shrimp. Dis Aquat Organ. 2004;60(1):85-8.
6. Osaka R, Kobayashi N, Shimada K, Ishii A, Oka N, Kondo K. VP26, a herpes simplex virus type 1 capsid protein, increases DNA methylation in COASY promoter region. Brain, Behavior, & Immunity-Health. 2022;26:100545.
7. Xie X, Yang F. White spot syndrome virus VP24 interacts with VP28 and is involved in virus infection. J Gen Virol. 2006;87(7):1903-8.
8. Dinesh S, Sudharsana S, Mohanapriya A, Itami T, Sudhakaran R. Molecular docking and simulation studies of Phyllanthus amarus phytocompounds against structural and nucleocapsid proteins of white spot syndrome virus. Biotech. 2017;7(5):353.
9. Molla MHR, Aljahdali MO. Identification of phytochemical compounds to inhibit the matrix-like linker protein VP26 to block the assembles of white spot syndrome virus (WSSV) envelope and nucleocapsid protein of marine shrimp: In silico approach. Journal of King Saud University-Science. 2022;34(8):102346.
10. Thomford NE, Senthebane DA, Rowe A, Munro D, Seele P, Maroyi A, et al. Natural products for drug discovery in the 21st century: innovations for novel drug discovery. Int J Mol Sci. 2018;19(6):1578.
11. Harvey AL. Natural products in drug discovery. Drug Discovery Today. 2008;13(19-20):894-901.
12. Rezaei M, Soltani M, Alipoor E, Rezayat SM, Vasheghani-Farahani A, Yaseri M, et al. Effect of nano-curcumin supplementation on angina status, and traditional and novel cardiovascular risk factors in overweight or obese patients with coronary slow flow phenomenon: a randomized double-blind placebo-controlled clinical trial. BMC Nutr. 2024;10(1):73.
13. Koohpeyma F, Khodaparast Z, Salehi S, Danesh S, Gheshlagh FM, Naseri A, et al. The ameliorative effects of curcumin nanomicelle on testicular damage in the mouse model of multiple sclerosis. BMC Complement Med Ther. 2024;24(1):200.
14. Praditya D, Kirchhoff L, Brüning J, Rachmawati H, Steinmann J, Steinmann E. Anti-infective properties of the golden spice curcumin. Front Microbiol. 2019;10:912.
15. Zhao P, Feng L, Jiang W, Wu P, Liu Y, Ren H, et al. Unveiling the emerging role of curcumin to alleviate ochratoxin A-induced muscle toxicity in grass carp (Ctenopharyngodon idella): in vitro and in vivo studies. J Anim Sci Biotechnol. 2024;15(1):72.
16. Nicoliche T, Bartolomeo CS, Lemes RMR, Pereira GC, Nunes TA, Oliveira RB, et al. Antiviral, anti-inflammatory and antioxidant effects of curcumin and curcuminoids in SH-SY5Y cells infected by SARS-CoV-2. Sci Rep. 2024;14(1):10696.
17. Alkhathami AG, Alshahrani MY, Alshehri SA, Nasir N, Wahab S. Curcumin as a potential inhibitor of TGFβ3 computational insights for breast cancer therapy. Sci Rep. 2025;15(1):2871.
18. Soriano-Díaz I, Ortí E, Giussani A. On the Importance of Ligand-Centered Excited States in the Emission of Cyclometalated Ir(III) Complexes. Inorg Chem. 2021;60(17):13222-32.
19. Patil R, Das S, Stanley A, Yadav L, Sudhakar A, Varma AK. Optimized hydrophobic interactions and hydrogen bonding at the target-ligand interface leads the pathways of drug-designing. PLoS One. 2010;5(8):e12029.
20. Dondapati[1] RS, Agarwal R. Overview of GROMACS. Molecular Dynamics Simulation of Nanocomposites using BIOVIA Materials Studio, Lammps and Gromacs. 2025:76.
21. Sousa da Silva AW, Vranken WF. ACPYPE - AnteChamber PYthon Parser interfacE. BMC Res Notes. 2012;5(1):367.
22. Megahed AA, Barakat A, Embaby AA, Mohamed SH, Sadik AS, Elshaer NA. Antiviral activity of turmeric (Curcuma longa) against potato virus Y: in silico molecular docking

analysis. Beni-Suef University J Basic Appl Sci. 2025;14(1):97.
23. Suravajhala R, Parashar A, Choudhir G, Kumar A, Malik B, Nagaraj VA, et al. Molecular docking and dynamics studies of curcumin with COVID-19 proteins. Netw Model Anal Health Inform Bioinform. 2021;10(1):44.
24. Srivastava AK, Kumar V, Roy BK. Insights from the molecular docking of curcumin to the virulent factors of Helicobacter pylori. Bioinformation. 2015;11(10):447-53.
25. Rampogu S, Lee G, Park JS, Lee KW, Kim MO. Molecular Docking and Molecular Dynamics Simulations Discover Curcumin Analogue as a Plausible Dual Inhibitor for SARS-CoV-2. Int J Mol Sci. 2022;23(3).
26. Erman B. Effects of ligand binding upon flexibility of proteins. Proteins. 2015;83(5):805-8.
27. Wankowicz SA, de Oliveira SH, Hogan DW, van den Bedem H, Fraser JS. Ligand binding remodels protein side-chain conformational heterogeneity. Elife. 2022;11.
28. Hollenbeck JJ, McClain DL, Oakley MG. The role of helix stabilizing residues in GCN4 basic region folding and DNA binding. Protein Sci. 2002;11(11):2740-7.
29. Yasuda T, Shigeta Y, Harada R. Efficient Conformational Sampling of Collective Motions of Proteins with Principal Component Analysis-Based Parallel Cascade Selection Molecular Dynamics. J Chem Inf Model. 2020;60(8):4021-9.
30. Liu K, Watanabe E, Kokubo H. Exploring the stability of ligand binding modes to proteins by molecular dynamics simulations. J Comput Aided Mol Des. 2017;31(2):201-11.